

### Two-Dimensional Interaction of Ion-Acoustic Solitons

P. A. Folkes,<sup>(a)</sup> H. Ikezi, and R. Davis<sup>(b)</sup>  
*Bell Laboratories, Murray Hill, New Jersey 07974*  
 (Received 23 May 1980)

The two-dimensional nonlinear interaction of two planar ion-acoustic solitons has been studied experimentally. When the angle between the wave vectors of the two interacting solitons is small and the soliton amplitudes approach a critical value, a resonant three-soliton interaction occurs.

PACS numbers: 52.35.Mw, 52.35.Dm, 52.35.Fp

Experimental studies of ion-acoustic solitons in the last decade have revealed that the behavior of solitons in one spatial dimension is well described by the Korteweg-de Vries equation.<sup>1</sup> The interaction of solitons in two and three dimensions is a problem of current interest. Recently, Ze *et al.*<sup>2</sup> have found that two interacting spherical ion-acoustic solitons produce a new nonlinear wave pulse. Although they speculated that this new wave was a consequence of the resonant interaction discussed by Newell and Redekopp,<sup>3</sup> no evidence of a resonance effect was presented. Yajima *et al.*<sup>4</sup> have found an explicit solution for two interacting planar solitons propagating in differ-

ent directions. In this Letter, we present the first experimental evidence which confirms a resonant three-soliton interaction and provides a quantitative comparison to the theory.

Before describing our experiment, we summarize the properties of solutions obtained in Ref. 4. We consider two planar solitons characterized by the density perturbations,  $\tilde{n} = \delta n \operatorname{sech}^2(\vec{k}_i \cdot \vec{r} - \omega t)$  ( $i = 1$  and  $2$ ), which propagate in the directions of the vectors  $\vec{k}_1$  and  $\vec{k}_2$ . These two planar solitons intersect and interact nonlinearly. Under these circumstances, a stationary-state expression for the density perturbation of the interacting solitons can be written as

$$\frac{\tilde{n}}{n_0} = \frac{4}{E^2} \frac{\delta n}{n_0} \left\{ \exp(2\theta_1) + \exp(2\theta_2) + 4 \sin^2\left(\frac{1}{2}\psi\right) \exp[2(\theta_1 + \theta_2)] + A[4 \cos^2\left(\frac{1}{2}\psi\right) + \exp(2\theta_1) + \exp(2\theta_2)] \exp[2(\theta_1 + \theta_2)] \right\}, \tag{1}$$

where

$$E = 1 + \exp(2\theta_1) + \exp(2\theta_2) + A \exp[2(\theta_1 + \theta_2)], \tag{2}$$

and for small  $\psi$ ,

$$A = \psi^2 / [\psi^2 - 8(\delta n/n_0)], \tag{3}$$

where  $\psi$  is the angle between  $\vec{k}_1$  and  $\vec{k}_2$ ,  $\theta_i = \vec{k}_i \cdot \vec{r} - \omega t$ , and  $n_0$  is the background plasma density. We consider only the case in which two solitons have equal amplitudes  $\delta n$ , where  $\delta n/n_0 = 6k^2/k_D^2$ ,  $k = |\vec{k}_1| = |\vec{k}_2|$ ,  $\omega/k = C_s(1 + \delta n/3n_0)$ ,  $C_s$  is the ion-acoustic speed, and  $k_D$  is the Debye wave number. When  $\delta n/n_0$  approaches a critical value  $\delta n_r/n_0 \equiv \psi^2/8$ , the parameter  $A$  becomes infinite, indicating that the resonance, discussed in Refs. 3 and 4, occurs.

Figure 1 shows equal-amplitude contour plots of Eq. (1) for two different cases,  $\delta n/\delta n_r = 0.2$  and  $0.998$ , when  $\psi = \pi/6$  and  $t = 0$ . The density perturbation propagates in the  $x$  direction with a speed  $\omega/k \cos(\psi/2)$  without changing the shape of its structure. When  $\delta n/\delta n_r = 0.2$ , the two solitons superimpose linearly. However, when  $\delta n/\delta n_r = 0.998$ , which is near resonance, the maximum

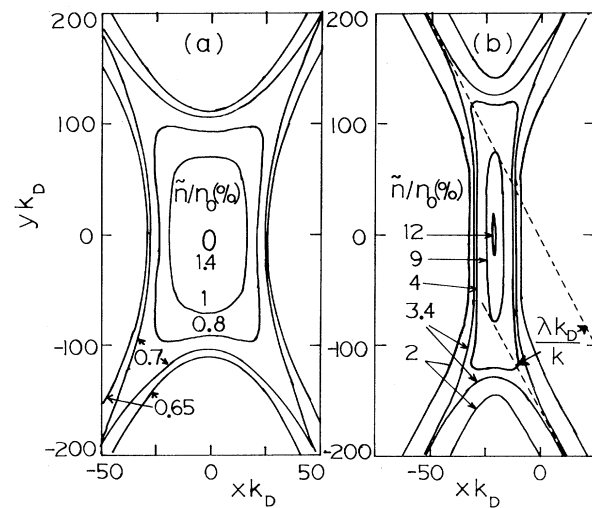


FIG. 1. Equal-amplitude contour plot of Eq. (1) when (a)  $\delta n/\delta n_r = 0.2$ ,  $\delta n/n_0 = 0.00685$ ; (b)  $\delta n/\delta n_r = 0.998$ ,  $\delta n/n_0 = 0.0342$ .

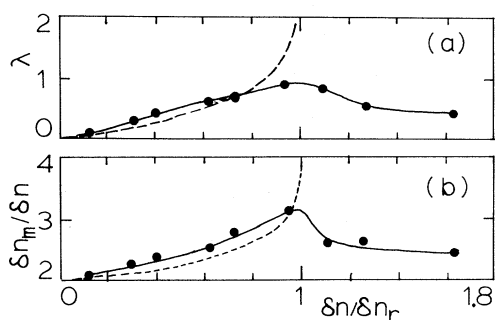


FIG. 2. Theoretical (dotted lines) and experimentally measured (solid lines) plots of (a) the phase shift and (b) the amplitude enhancement ratio, as a function of the ratio of soliton amplitude to the critical amplitude,  $\delta n/\delta n_r$ .  $\psi = \pi/6$ .

amplitude  $\delta n_m$  occurring near the center of the structure is  $1.75(2\delta n)$  indicating a nonlinear interaction. A new large-amplitude soliton is created and causes the phase shift  $\lambda$ , defined in Fig. 1.

The phase shift  $\lambda$  and the amplitude enhancement ratio  $\delta n_m/\delta n$  are plotted in Fig. 2 as a function of  $\delta n/\delta n_r$ . As  $\delta n$  approaches  $\delta n_r$ ,  $\lambda$  logarithmically goes to infinity indicating that the width of the new soliton in the  $y$  direction becomes large. The quantity  $\delta n_m/\delta n$  approaches 4 as  $\delta n$  goes to  $\delta n_r$ , but decreases to 2 when  $\delta n/\delta n_r$  is small. When  $\delta n > \delta n_r$ , the theory predicts an (unphysical) singular soliton.

The experiment was carried out in a double-plasma device.<sup>5</sup> The device consists of two identical, electrically isolated, conducting vacuum chambers each producing a plasma by electrical discharge in argon gas. A fine mesh grid (40 lines/cm) which is negatively biased separates the two plasmas. The grid consists of two planar surfaces at an angle to each other joined along a common edge (see Fig. 3). The application of a half-sinusoidal voltage pulse between the chambers launches two compressive ion-acoustic wave pulses<sup>5</sup> propagating normal to the planar grid surfaces. The wave pulses steepen to form solitons. The angle between the soliton propagation vectors,  $\vec{k}_1$  and  $\vec{k}_2$ , is equal to the angle between the vectors normal to the two planar grid surfaces. Density perturbations are measured by detecting the electron saturation current with a planar Langmuir probe having dimensions  $1 \times 8$  mm<sup>2</sup>. The ion distribution is also monitored using an electrostatic energy analyzer. We employ a signal sampling method to plot the wave perturbation as a function of space for given delay times after the wave excitation pulses are applied. The typi-

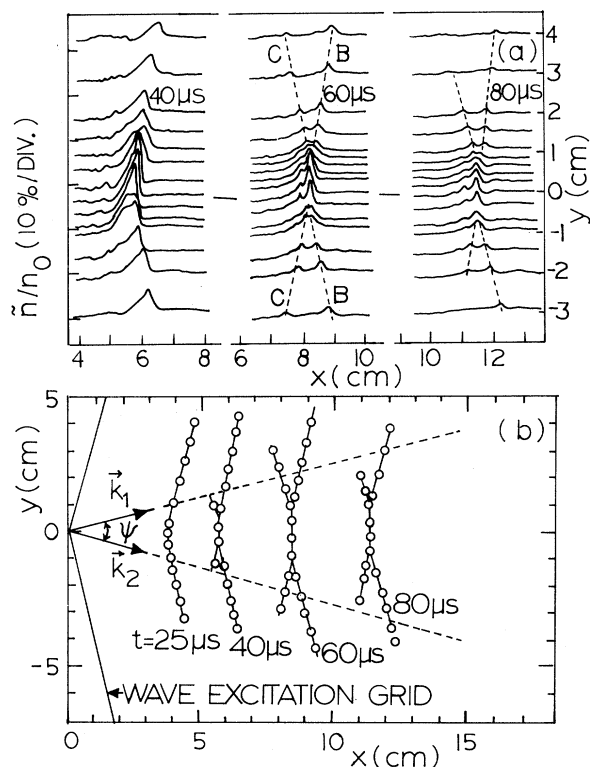


FIG. 3. (a) The spatial structure of the density perturbation is shown at  $t = 40, 60,$  and  $80 \mu\text{s}$  when  $\psi = \pi/6$ . (b) A scale diagram is shown of the wave excitation grid and contours of the soliton peaks from Fig. 3(a) at different times  $t$ . The space between the two dotted lines is the interaction zone.

cal plasma parameters are: plasma density  $n_0 = 10^9$  cm<sup>-3</sup>; electron temperature  $T_e = 1.7-2$  eV; ion temperature  $T_i = 0.1$  eV; argon-gas pressure  $p = (2-5) \times 10^{-4}$  Torr. The ion-acoustic speed is typically  $1.5 \times 10^5$  cm/sec. The Debye length  $\lambda_D = 2.5 \times 10^{-2}$  cm. Under these conditions, the plasma is almost collisionless.

Figure 3(a) shows the experimentally measured spatial evolution of the two-dimensional wave structure at different times. The wave excitation pulse is applied at  $t = 0$ , and the coordinate system  $(x, y)$  used in the following description is defined in Fig. 3(b). The compressional pulse already steepens and starts forming a soliton near  $y = 0$  at  $t = 40 \mu\text{s}$ . The background density in front of the wave pulse is slightly larger than the density behind the pulse. Energy analyzer measurements show that this density difference is due to ions reflected by the electrostatic potential associated with the wave. At  $t = 60 \mu\text{s}$ , we observe the wave structure similar to the one shown in Fig. 1(b); a large-amplitude soliton occurs at  $x = 8.0$

cm and  $|y| \lesssim 1$  cm and its peak splits into two solitons at  $|y| \gtrsim 1.2$  cm (the dashed lines indicate peak position). As the wave propagates, the amplitude damps because of loss of energy to the reflected ion. As a result, the soliton width increases, but the wave structure is maintained.

The contours of the soliton peak shown in Fig. 3(b) indicate that the structure we are considering appears in a zone where the two waves excited by the two parts of the grid are overlapping. The soliton peak labeled C in Fig. 3(a) is smaller than the one labeled B because it is closer to the boundary of the overlapping zone. In this zone, the propagation velocity in the  $x$  direction is larger than  $C_s$  and agrees approximately with the theoretical value.

We observe a phase shift  $\lambda$ , in Fig. 3(b) after  $40 \mu\text{s}$ . As the amplitude damps the data (not shown in the figure to avoid confusion) shows that  $\lambda$  increases to a maximum at  $60 \mu\text{s}$  where the resonance condition  $\delta n/n_0 = \psi^2/8$  is satisfied. The phase shift decreases with further attenuation of amplitude. The data points for  $\lambda$  shown in Fig. 2(a) agree with the theoretical values except when  $\delta n \approx \delta n_r$ . The phase shift does not become infinite because the condition  $\delta n = \delta n_r$  is met for only a very short period of time.

The amplitude enhancement ratio  $\delta n_m/\delta n$  is about 2 when  $\delta n/\delta n_r \ll 1$  and increases with  $\delta n$  [see Fig. 2(b)]. The largest observed value of  $\delta n_m/\delta n$  is about 3.1, which occurs near the resonance amplitude,  $\delta n \approx \delta n_r$ . We have observed the wave structure similar to the one shown in Fig. 3(a) even when  $\delta n > \delta n_r$  where Ref. 4 predicts only an unphysical, singular soliton. However, the actual wave structure is complicated. In order to produce large-amplitude solitons with  $\delta n > \delta n_r$ , we need to use a wider initial pulse which evolves into several solitons near  $y=0$ . In this case, we observe a splitting of each soliton into two pulses at larger  $|y|$  and these pulses then interact. We find experimentally that both  $\lambda$  and  $\delta n_m/\delta n$  for  $\delta n > \delta n_r$  are smaller than those values when  $\delta n \approx \delta n_r$ .

To check the angular dependence of the resonant interaction, we also made measurements for  $\psi = \pi/2$  and  $\psi = \pi/12$ . For the case  $\psi = \pi/12$ , we did not observe a distinct splitting of the central, large-amplitude soliton. This is probably due to the fact that the interaction zone is very narrow when  $\psi = \pi/12$ , and the soliton amplitude decreases sharply outside the zone.

When  $\psi = \pi/2$ , we observed a different spatial structure as shown in Figs. 4(a) and 4(b). For the case shown in Fig. 4(a), a large-amplitude

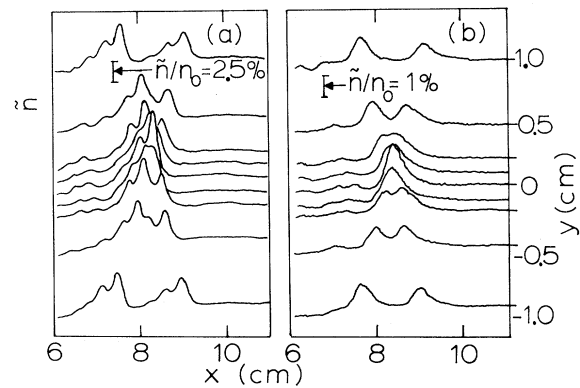


FIG. 4. Two-dimensional density perturbation showing the case of a linear interaction for  $\psi = \pi/2$ : (a)  $\delta n/n_0 = 0.04$ ; (b)  $\delta n/n_0 = 0.01$ .

excitation pulse is used and two sets of multiple solitons excited by each planar grid surface are observed. In this case, the amplitude enhancement ratio observed equals two. No phase shift was observed. A linear superposition of the two solitons occurs at  $y=0$ . Therefore no new soliton is observed. Figure 4(b) shows the same behavior for a small-amplitude soliton. These results agree with the theory which predicts a linear interaction at large  $\psi$ .

It should be noted that the theory describes only a stationary state soliton structure, but it does not treat the temporal evolution of the wave. We have shown that this stationary state is developed from a particular set of initial conditions.

<sup>(a)</sup>Also at Department of Applied Physics and Nuclear Engineering, Columbia University, New York, N. Y. 10025.

<sup>(b)</sup>Also at Massachusetts Institute of Technology, Cambridge, Mass. 02139.

<sup>1</sup>H. Ikezi, in *Solitons in Action*, edited by K. E. Lonngren and A. Scott (Academic, New York, 1978), pp. 123-164.

<sup>2</sup>F. Ze, N. Hershkowitz, C. Chan, and K. Lonngren, *Phys. Rev. Lett.* **42**, 1747 (1979), and *Phys. Fluids* **23**, 1155 (1980).

<sup>3</sup>A. C. Newell and L. G. Redekopp, *Phys. Rev. Lett.* **38**, 377 (1977).

<sup>4</sup>N. Yajima, M. Oikawa, and J. Satsuma, *J. Phys. Soc. Jpn.* **44**, 1711 (1978).

<sup>5</sup>R. J. Taylor, K. R. MacKenzie, and H. Ikezi, *Rev. Sci. Instrum. Methods* **43**, 1675 (1972).